An Improved On-line Contingency Screening for Power System Transient Stability Assessment

Tilman Weckesser*, Hjörtur Jóhannsson†, Mevludin Glavic*, and Jacob Østergaard†

* Dept. Elect. Engineering & Comp. Science at the University of Liège, 4000 Liège, Belgium.

† Centre for Electric Power and Energy, Dept. of Elect. Engineering, Technical University of Denmark, 2800 Lyngby, Denmark.

This paper presents a contingency screening method and a framework for its on-line implementation. The proposed method carries out contingency screening and on-line stability assessment with respect to first-swing transient stability. For that purpose, it utilizes the single machine equivalent method and aims at improving the prior developed contingency screening approaches. In order to determine vulnerability of the system with respect to a particular contingency, only one time-domain simulation needs to be performed. An early stop criteria is proposed so that in a majority of the cases the simulation can be terminated after a few hundred milliseconds of simulated system response. The method's outcome is an assessment of the system's stability and a classification of each considered contingency. The contingencies are categorized by exploiting parameters of an equivalent one machine infinite bus system. A novel island detection approach, appropriate for an on-line application since it utilizes efficient algorithms from graph theory and enables stability assessment of individual islands, is also introduced. The New England and New York system as well as the large-scale model of the Continental-European interconnected system are used to test the proposed method with respect to assessment accuracy and computation time.

1 Introduction

The production pattern in today's power system with high shares of power generation from renewable energy sources, situation expected to be even more pronounced in the future, may change fast with increased fluctuations of the power system's operating point. This requires a fast on-line dynamic security assessment (DSA) method [1]. Most of the current methods for stability assessment are based on extensive off-line computations and, consequently, may no longer be sufficient. A fast on-line DSA is of crucial importance [2]. A wide range of approaches and methods have been proposed for DSA [3] and fast contingency screening. In [4] the authors discussed various severity indices for dynamic security analysis and ranking of contingencies. The indices are based on coherency, transient energy conversion or on dot products of certain system states. In the approach, a detailed time-domain simulation is carried out until 500 ms after fault clearance. Then the indices are computed to determine stability and to rank the respective contingency. In [5] a screening method utilizing the transient energy function was proposed, where the aim is to filter non-severe disturbances. In the recent publication [6], a contingency screening and ranking approach is proposed, which applies a homotopy-based approach to identify the controlling unstable equilibrium point. Another case screening approach based on the extended equal area criterion (EEAC) was presented in [7]. The main idea

The Version of Record of this manuscript has been published and is available in Electric Power Components and Systems 02 May 2017 http://www.tandfonline.com/10.1080/15325008.2017.1310953.

was again to filter the majority of stable cases with data gathered just after fault clearance and to carry out detailed time domain simulation combined with the integrating EEAC on the remaining yet undetermined cases. In [8] the authors propose a contingency, filtering, ranking, and assessment method based on single machine equivalent (SIME). The method consists of two blocks. The first block filters stable contingencies and the second block ranks and assesses the remaining possible harmful contingencies according to their estimated critical clearing times (CCTs). For that purpose, up to two time-domain simulations per contingency are carried out. The fast contingency screening approach presented in [9] is as well based on SIME. The authors introduce a new index for grouping of the generators and a contingency classification based on the power-angle shape of the one-machine infinite bus (OMIB) equivalent. For that purpose, the method carries out one to three time-domain simulations per contingency with varying fault clearing time. Alternatively, to these presented contingency screening methods, which are executed periodically, the advent of wide-area measurement systems in power systems enabled the development of transient stability prediction methods utilizing real-time synchronized phasor measurements. In the early reference [10] the authors propose a method to predict transient rotor swings, which uses a fuzzy hyperrectangular composite neural network and post-contingency phasor measurements to determine stability. In the recent reference [11] a method for transient stability prediction and mitigation is presented. The method uses real-time measurements provided from phasor measurement units (PMUs) and an artificial neural network (ANN) to detect stability or instability of the power system. If instability is detected, a remedial action scheme is activated.

Currently, a revived interest in direct methods for transient stability assessment can be seen. In [12] the concept of using a Lyapunov function is revisited, in [13] the BCU method is further developed and in [14] the concept of SIME is utilized.

In this paper, a stability assessment and contingency screening method is proposed, which assesses the system's transient stability and whose performance is suitable for an on-line application. The proposed method could be part of an extensive DSA toolbox and builds on prior developed approaches based on SIME, which was chosen since in [15] it was identified as being the fastest direct transient stability assessment (TSA) method. In this paper, four contributions are presented. The first one is the proposal of early stopping criteria, which allow an early stability determination and, hence, an early termination of the needed time-domain simulation. The second contribution is that to determine stability of the power system and to classify a contingency only one simulation is required, where the fault clearing time is chosen corresponding to the actual settings of the protective relays. This is made possible due to the further development of an approach of classifying contingencies by considering the power-angle shape of the respective OMIB. The third contribution is a novel method to detect the formation of islands as well as to identify the generators and loads in islands based on an efficient algorithms from graph theory making it suitable for on-line applications. To validate the proposed approach, it is tested on a real-life large-scale power system, which is considered to be the fourth contribution.

2 Method

The proposed TSA and contingency screening method is assumed to be executed periodically several times per day or triggered by certain events. These events may be e.g. larger changes in the generation/consumption pattern or occurrences of structural changes in the system. It should be noted that the method does not aim at predicting the transient response of the system after the occurrence of a fault, instead the method carries out a contingency screening to ensure system stability with respect to a given set of contingencies. Figure 1 shows the block diagram of the proposed method integrated into

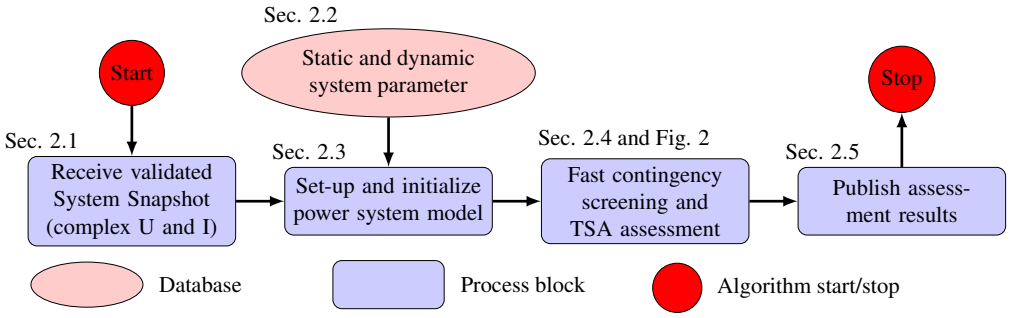

Figure 1. Block diagram of the proposed screening and assessment method integrated into a framework for online assessment

an on-line DSA framework, similar to the power system simulation platform described in [16]. In the following subsections, each block will be described in more detail.

2.1 System Snapshot

This block reads validated system snapshots consisting of complex bus voltages from all system buses as well as currents flowing in and out of each transmission line or transformer. The snapshot represents the pre-fault quasi-steady state system condition and is determined from wide-area measurements or a fast state estimator. If the speed of the state estimator is not sufficient and PMUs are only installed at a limited number of buses in the system, methods such as the one described in [17] can be used to track the network state and to provide system snapshots in real-time. The latest system snapshot is considered to represent the system's pre-fault condition and, hence, is later used to initialize the time-domain simulations.

2.2 Static and dynamic system parameters

The database contains the model parameter for all electric components in the monitored power system. It is assumed that the provided parameters are sufficient to represent the power system components (e.g. generators, transformers, loads, etc.) with enough detail to allow accurate simulation of the transient system response. This means that e.g. the rotor dynamics of synchronous generators are at least represented by a 4^{th}-order model, which was suggested in [18].

2.3 Power system model

In this block, the obtained system snapshot and the system parameters are utilized to set-up a power system model including the admittance matrix $\mathbf{Y}$. Furthermore, the data are used to initialize the model to represent the current system state. Finally, a list of contingencies is generated which will be used in the screening and stability assessment.

2.4 Fast contingency screening and TSA assessment

Figure 2 shows the block diagram of the proposed on-line contingency screening and stability assessment algorithm.

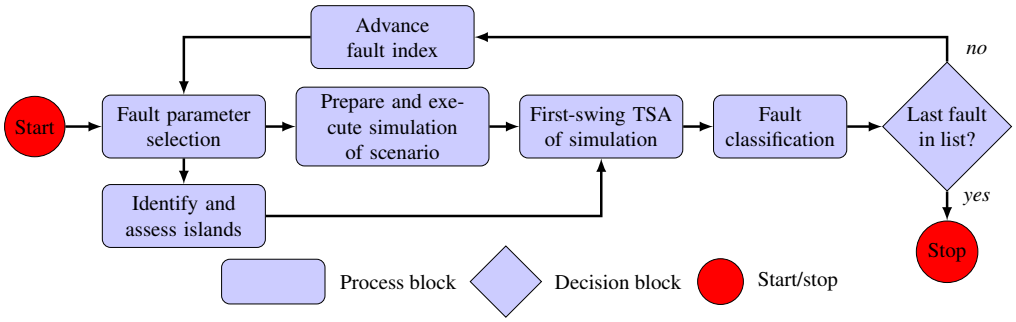

Figure 2. Block diagram of the fast contingency screening and TSA assessment algorithm

2.4.1 Fault parameter selection First, the parameters of the next fault on the contingency list are extracted from the system model. These include type of fault (e.g. three-phase short circuit), fault location, fault clearing time and fault clearance. The fault location corresponds to the bus or branch where the fault occurs. The fault clearing time is given by the protection relays in the vicinity of the fault. The fault clearance provides information on e.g. the breakers opened to isolate the fault.

2.4.2 Prepare and execute simulation After the fault parameters have been determined, the time-domain simulation of the scenario can be prepared. The model database provides the needed parameters of each component to set-up the dynamic models and the latest system snapshot is utilized to initialize the power system model.

2.4.3 Identify and assess islands In this block it is determined, if the fault and its clearance are causing a splitting of the power system into separated islands. Algorithm 1 shows the proposed island identification and assessment method as pseudo code. In the following the algorithm will be explained in detail. In order to refer to parts of the algorithm, the text will refer to particular line numbers in the algorithm (AL).

As input the method requires the system's admittance matrix $\mathbf{Y}$, the branches b tripped due to fault clearance, a list of *buses* in the system and data of *generators* as well as *loads*. In order to use the efficient algorithms from graph theory, the power grid model needs to be converted into a graph. For that purpose, $\mathbf{Y}$ is modified according to the assumed fault clearance by calling the function *updateY* (see $AL2$). Assuming that the respective fault is cleared by disconnecting the branches b, the function computes the individual branch admittances and adds them to the respective off-diagonal entries as well as it subtracts them from the diagonal entries of the buses connected by the respective branch. If the only direct connection between two buses was one of the branches, the corresponding off-diagonal entries will be equal to zero after the modification, which indicates that there is no longer a branch connecting the two buses. Consequently, the updated admittance matrix $\mathbf{Y_{up}}$ can easily be converted into a corresponding adjacency matrix of an undirected graph g by generating a copy of $\mathbf{Y_{up}}$ and setting all non-zero values equal to one. The conversion is performed by the function *convertY* (see $AL3$), which returns the corresponding graph g. Subsequently, the efficient algorithms from graph theory can be applied to identify, if the network is still connected or if islands were formed. A recursive depth-first search (DFS) algorithm (see e.g. [19]) is utilized for these purposes. In $AL4-9$ for each tripped branch the DFS is executed starting at the $b[n].from$, which is the from-bus of the n^{th} tripped branch, and with the target $b[n].to$, which is the to-bus of the n^{th} tripped branch. The DFS function investigates g

Algorithm 1 Algorithm to identify and assess islands

```
1: function ISLANDS(Y, b, generators, loads, buses)
2:     Y_up =updateY(Y,b)
3:     g = convertY(Y_up)
4:     for n=1:len(b) do
5:         [sflag, explored] =DFS(g, b[n].from, b[n].to)
6:         if sflag ≠ 1 then
7:             break
8:         end if
9:     end for
10:    if sflag ≠ 1 then
11:        k = 1
12:        isl[k] = explored
13:        gen[k] = storeG(explored, generators)
14:        load[k] = storeL(explored, loads)
15:        rbuses = buses − explored
16:        while rbuses do
17:            next = rbuses[1]
18:            k = k + 1
19:            [sflag, explored] =DFS(g, next)
20:            isl[k] = explored
21:            gen[k] = storeG(explored, generators)
22:            load[k] = storeL(explored, loads)
23:            rbuses = rbuses − explored
24:        end while
25:    end if
26:    return isl, gen, load
27: end function
```

to determine if another direct or an indirect connection exists between the two buses. If a connection is found, the function returns the success flag $sflag$ equal to 1, else it returns $sflag = 0$ and the for-loop is exited. If the network was split $sflag \neq 0$, the algorithm begins to identify the created islands (see $AL10$ ff.). Besides the success flag, DFS also returns a list of the *explored* buses. In case that no connection between the respective from- and to-bus was found, *explored* contains a list of all buses in the island. The list is stored in the output variable *isl* (see $AL12$). Subsequently, the functions *storeG* and *storeL* determine, which generators and loads are located in the identified island. The resulting lists of generators and loads are stored in the output variables *gen* and *load*, respectively (see $AL13$ & 14). Then the *explored* buses are removed from the list *buses* and the identification of islands is continued by performing depth-first searches starting from the first bus of the list of remaining buses *rbuses*. It is terminated when the list *rbuses* is empty (see $AL16 - 24$).

The algorithm's output indicates if islands were created. If the power system was split, it provides the buses, generators and loads in each island.

2.4.4 First-swing TSA of simulation results The simulation as well as the island identification and assessment results are forwarded to the TSA block, where in each time step transient stability of the system or, if fault clearance created islands, of each island is assessed using the preventive SIME method.

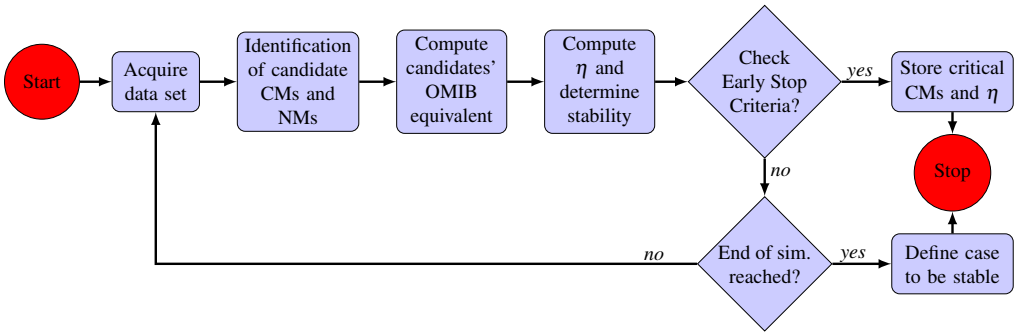

Figure 3. First-swing transient stability assessment algorithm

Preventive SIME is a hybrid TSA method, which combines the advantages of both detailed time-domain simulation and the equal area criterion (EAC). In [8] a detailed description of the method can be found and [20] recently presented a discussion of the achievements and prospects of Emergency SIME. SIME is derived based on the assumption that the post-fault dynamics of a multi-machine power system can be represented by a suitable OMIB equivalent. In this process, the machines are split into a group of Critical and Non-critical Machines (CMs and NMs, respectively). The critical group contains those machines which are likely to lose synchronism and the non-critical group the rest of the machines. If a harmful contingency has been identified, the CMs can be immediately considered in the determination of preventive/remedial actions. After the OMIB has been determined, the EAC can be applied to assess transient stability. Figure 3 shows the proposed first-swing TSA algorithm, which is described in more detail in the following.

Acquire data set: In order to assess transient stability, the method requires a system snapshot provided by PMUs or a fast state estimator as well as time invariant parameters, such as the inertia coefficient of each generator and, if islands were created, the generators in each island, which is provided by the function described in Sec. 2.4.3. Apart from that the method needs at least three successive data sets of rotor angles, rotor speeds, mechanical powers and electrical active powers from all generators in the post-fault configuration obtained from time-domain simulation. In this implementation of the method up to six successive data sets are considered.

Identification of candidate critical and non-critical machines: In order to determine an OMIB equivalent, the generators are split into the two groups (CMs and NMs, respectively). Candidate CMs and NMs are identified under consideration of the evolution of the generators' individual rotor angles. For that purpose, the rotor angles are predicted some time ahead (e.g. 100 ms) using Taylor series expansion. As described in [8], the candidate CMs are then identified based on the predicted rotor angles. The approach is visualized in Fig. 4. In this implementation, in each assessment step up to three candidate CM and NM groups per island were considered.

Compute candidates' OMIB parameters: In the next step, the gathered simulation data are used to formulate the OMIB equivalent, which represents the dynamics between a group of CMs and NMs. This is done for each candidate group of CMs and NMs in each island. The detailed computation of the OMIB parameters are described in [8]. The proposed method is an extension of SIME, where the OMIB dynamics are driven by the swing equation, and inherits all good characteristic of that method. The resulting OMIB is characterized by its rotor angle $\delta(t)$, speed $\omega(t)$, inertia coefficient M and acceleration power $P_a(t)$.

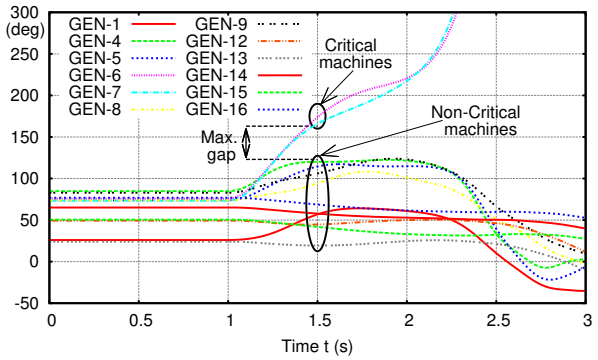

Figure 4. Visualization of the concept of identifying the CMs and NMs from the rotor angle response of the generators.

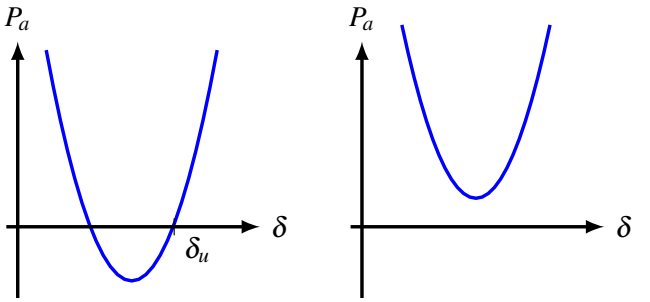

(a) Case I: stable or unstable (b) Case II: definitely unstable

Figure 5. Considered $P_a(\delta)$-curve shapes

Computation of the stability margin and determination of stability: By employing the EAC, the determined parameter of the candidate OMIB allow to compute the transient stability margin η, which is negative for an unstable and positive for a stable case [8]:

$$\eta = -\int_{\delta_i}^{\delta_u} P_a d\delta - 1/2\, M\omega_i^2 \tag{1}$$

where δ_i and ω_i correspond to $\delta(t_i)$ and $\omega(t_i)$. δ_u is the angle where the following instability conditions are met:

$$P_a(\delta_u) = 0 \text{ and } \dot{P}_a(\delta_u) > 0 \tag{2}$$

In the Preventive SIME method the angle δ_u is estimated through an approximation of the $P_a(\delta)$-curve of the OMIB. For this purpose, (at least) three successive data sets of the OMIB, consisting of P_a and δ, are used to compute a quadratic approximate of the curve.

The two curves shown in Fig. 5 represent valid approximation of the $P_a(\delta)$-curve and the stability margin computation is straight forward. In Case I (see Fig. 5a), the angle δ_u is found employing the condition in (2) and the stability margin is computed with (1). When the OMIB does not have an equilibrium point, meaning that the estimated $P_a(\delta)$-curve does not intersect $P_a = 0$, as shown in Case II in Fig. 5b, a stability margin cannot be computed with (1). However, in that case, as suggested in [8], the kinetic energy of the OMIB can be used to represent the negative stability margin and can be

Table 1. Classification of contingencies (where g: number of generators and l: number of loads in an island)

Classifier	η	$\frac{dP_a}{d\delta}\big\vert_{\delta=\delta_r}$	ω	Number of generators & loads
Definitely Unstable (DU)	–	–	–	–
	–	–	–	$g \geq 1;\ l = 0$
Unstable (U)	< 0	–	–	–
Not Classifiable (NC)	–	–	–	$g = 1;\ l \geq 1$
Marginal Stable (MS)	> 0	> 0	–	$g \geq 2;\ l \geq 1$
	–	> 0	< 0	$g \geq 2;\ l \geq 1$
Stable (S)	> 0	< 0	–	$g \geq 2;\ l \geq 1$
	–	< 0	< 0	$g \geq 2;\ l \geq 1$
Definitely Stable (DS)	–	–	$< \omega_{lim}$	$g \geq 2;\ l \geq 1$

computed as follows.

$$\eta = -1/2\, M\omega_i^2 \tag{3}$$

Early Stop Criteria: The time-domain simulation and the stability assessment can be stopped, when from the candidate OMIBs the most critical one is identified and the computed stability margin converged to a constant value. The most critical OMIB in an unstable case is either the one, which first crosses δ_u and, hence, the unstable equilibrium point (UEP), or the one, which first reaches the minimum of the $P_a(\delta)$-curve in case that no post-fault equilibrium exists. In a stable case, the most critical OMIB is the one, which is the last one to reach the return angle δ_r, where the following stability conditions are met.

$$P_a(\delta_r) < 0 \text{ and } \omega_r = 0 \tag{4}$$

In each simulation step, the candidate OMIBs in each island are assessed to identify the most critical OMIB. Once it has been identified, the assessment is continued until the stability margin converged to a constant value. When the two conditions are satisfied the stability margin and the CMs of the respective OMIB are stored and forwarded to the contingency classification block (see Fig. 2).

2.4.5 Classification of faults In order to classify the faults, a classification index is introduced. It utilizes characteristics of the approximated $P_a(\delta)$-curve and states of the OMIB at the time the early stop criteria were satisfied. Moreover, in certain cases it allows immediate classification of islands based on the number of generators and loads. The proposed classification builds on the approach presented in [9]. However, in order to improve performance and decrease the number of required simulations to one, the criteria for classification of the cases are changed. Additionally, the classification criteria were extended to allow assessment of power system islands. Table 1 shows the classification criteria, which , in the following, are described in detail. A contingency is classified to be Definitely Unstable (DU), if the $P_a(\delta)$-curve, as shown in Fig. 5b, does not intersect zero and a post-contingency equilibrium point does not exist. Moreover, in case of a splitting of the power system, a contingency is rated DU for an island, when it only contains generators ($g \geq 1$), but no loads ($l = 0$). A contingency is classified Unstable (U), if the determined stability margin is negative. If the most critical OMIB has reached its return angle δ_r and the angle is located on the side of the $P_a(\delta)$-curve, where $dP_a/d\delta > 0$, then the contingency is assessed to be Marginal Stable (MS). However, if δ_r lies on the side of the $P_a(\delta)$-curve, where $dP_a/d\delta < 0$, then it is classified Stable (S). A contingency

is only classified Definitely Stable (DS), if the relative rotor speed of all the candidate OMIBs after fault clearance are below a certain threshold (e.g. $\omega_{lim} < 0.1$ rad/s) or if the maximum simulation time was reached without identification of the most critical OMIB. Finally, if an island only contains one generator ($g = 1$) and loads ($l \geq 1$), the method cannot determine stability of the island, since no reference is available to determine loss of synchronism. Hence, it is categorized as Not Classifiable (NC). Table 1 summarizes the classifiers and the used criteria. The classification of the contingencies can be used to determine further assessment strategies. For example, NC or MS cases could be investigated in more detail e.g. with extensive time-domain simulation and DU cases could be prioritized, when determining preventive control actions.

2.5 Publish assessment results

After fault screening and TSA assessment, the obtained results are published (see Fig. 1) to make them available for other functions or methods, e.g. visualization tools or methods determining preventive controls. This may be realized through a platform similar to the one described in [16].

3 Results

3.1 Test system, cases and set-up

3.1.1 Test system Two test systems were employed to validate the presented screening method. The first test system is the New England and New York system described in [21], which consists of 68 buses and 16 generators. The loads are modelled as constant impedances in the time-domain simulation. The generators are represented by a sixth order model. They all have a simple excitation and voltage regulation system, as well as a thermal turbine/governor model. Moreover, all generators, but GEN-7 and GEN-14, are equipped with a power system stabilizer. The second test system demonstrates the performance on a large scale system. For that purpose, the ENTSO-E Dynamic Study Model (DSM), which was presented in [22] and which is available upon request[1], was chosen. The ENTSO-E DSM corresponds to the interconnected power system of Continental Europe. The model contains 24 625 buses and 1 013 generators. All loads were modeled as constant impedances in the time-domain simulation. Further details can be found in [22].

3.1.2 Test cases For the purpose of testing the on-line contingency screening method, a set of contingencies was defined. In the New England and New York test system, the set includes two three-phase fault scenarios per transmission line, where one time the fault is close to the from-bus and the second time the fault is close to the to-bus. This resulted in 172 cases. Furthermore, the method was tested with three different fault clearing times (50, 200 and 500 ms) to vary the total number of stable and unstable cases. These tests are in the following referred to as Test I, II and III, respectively.

In the ENTSO-E DSM, the contingency screening was carried out in the Spanish power system (in practice TSA is performed by individual transmission system operators). The transient stability of the 71 Spanish generators was assessed with respect to short-circuits lasting 500 ms on each of the 400 kV transmission lines in the Spanish power system. This resulted in 349 cases, which are subsequently referred to as Test IV.

In order to determine, if the stability assessment with the online screening method is correct, the result are compared against a reference. For this purpose, the rotor angle of the generators within an island are assessed at the end of the time domain-simulation

[1]The request form can be found here: https://www.entsoe.eu/publications/system-operations-reports/continental-europe/Initial-Dynamic-Model/Pages/default.aspx

Table 2. Performed tests and assessment results from time-domain simulation

Test	Clearing time $[ms]$	Number of stable	Number of unstable
Test I	50	168	40
Test II	200	137	71
Test III	500	55	153
Test IV	500	252	97

of 4 s, which is sufficient to ensure capturing of the first swing. If at the end of the simulation the rotor angle of at least two generators are more than 120° apart, then the island is identified to be unstable, else stable. This maximum angle was chosen, since it is a common setting for generator out-of-step protection [23]. The reference stability assessment results are shown in Table 2. It can be observed that the number of stable and unstable cases varies greatly. When the clearing time is chosen to be short (50 ms) the number of stable cases is significantly larger than the number of unstable cases. On the contrary, when the fault is assumed to be lasting long (fault clearing time of 500 ms), the number of unstable cases is larger than the number of stable cases. In this way, the method can be tested on a large number of stable as well as unstable cases. The total number of assessments is larger than the number of test cases, because in cases where the fault clearance leads to splitting of the system the stability of the individual islands is determined.

3.1.3 Test set-up The tests were carried out on a standard laptop with the following characteristics: Intel®Core™i7-4720HQ, 2.6 GHz, 16 GB DDR3 RAM, running on 64-bit Ubuntu Linux 16.04 LTS. The time-domain simulations were carried out using the software RAMSES developed at the Univ. of Liège [24], which employs decomposition and localization technics to speed up computations. The proposed method, shown in Fig. 1, was implemented in GNU Octave. The CPU times include all steps of the contingency screening. Due to the use of a fast external time-domain simulator and not an integrated numerical integrator, the system variables are not accessible during the simulation. Hence, the simulations are carried out for a fixed time (e.g. 4 s) and the trajectories of the needed system variables are stored in a file.

3.2 Contingency screening and stability assessment results

First, the accuracy of the method will be evaluated by comparing the stability assessment results with the reference. Second, the performance of the method will be presented in terms of the runtime. Finally, the classification results are presented and discussed.

3.2.1 Accuracy of the proposed method The accuracy will be presented by assessing the number of correctly identified stable/unstable cases. As a reference stability assessment results were extracted from time-domain simulations. For that purpose, simulations were run for 4 s, which is expected to be sufficient to investigate the first swing response, and a case is considered to be unstable, if at the end of the simulation the rotor angles of at least two generators deviate by more than 120°. The assessment result obtained with the proposed method is then compared to this reference. Table 3 shows the results of the accuracy assessment for the four different tests. First of all, it should be noted that the success rates of the proposed contingency screening method are very high. Between $89.09 - 98.41$ % of the stable cases are correctly identified by the proposed contingency screening method and the success rates for identifying unstable cases are even higher with $95.88 - 100.0$ %. The rate for identifying an unstable case being generally higher

Table 3. Accuracy of fast screening method

Test	Clearing time $[ms]$	Identified stable cases	Identified unstable cases
Test I	50	96.43%	100.00%
Test II	200	94.16%	98.59%
Test III	500	89.09%	100.00%
Test IV	500	98.41%	95.88%

corresponds to a slightly more conservative characteristics of the method. This is preferable to a progressive characteristic, which would have the undesirable effect of increasing the rate of unstable cases being wrongly assessed as stable.

3.2.2 Comparison of Type I errors In the following, the proposed improved method is compared to the original SIME method, which was presented in [8]. The original SIME method only allows to divide the individual cases into stable and unstable and does not inherently allow further differentiation. Hence, the methods are compared with respect to the probability of Type I errors (false positive) when determining stability. Table 4

Table 4. Comparison of probability of Type I errors

Test	System response	Assessment result	Original SIME	Improved approach
Test I	unstable	stable	0.7 %	0.0 %
	stable	unstable	26.4 %	13.0 %
Test II	unstable	stable	1.7 %	0.7 %
	stable	unstable	23.3 %	10.3 %
Test III	unstable	stable	2.2 %	0.0 %
	stable	unstable	6.2 %	3.8 %

shows the obtained results. It can be observed that the probability for Type I errors is generally lower in the improved approach. For example in Test I, when a case is identified to be unstable with the original SIME approach, the probability is 26.4 % that the system response is in fact stable. With the improved approach, the probability is approximately half.

3.2.3 Performance of the screening method The performance is assessed in two ways. First, the runtime of the implementation is assessed and, afterwards, the potential speed-up is estimated, for the case that the method is seamlessly integrated with a time-domain (T-D) simulator, which enables stopping the simulation when the early stop criteria are satisfied.

Performance with fixed simulation time: Table 5 displays the runtimes obtained in the four tests. It shows the total runtime and the average runtime per contingency for two setups. In the first setup, the time-domain simulation is included. In the second, the already simulated data are solely read and utilized for stability assessment. In the tests using the New England and New York system (Test $I - III$), the total runtimes including the simulation are in the range of 71.35 s to 87.76 s, which corresponds to an average runtime of $415 - 510$ ms per contingency. It can be observed, that the runtime increases with the fault clearing time and, consequently, with the number of unstable cases.

Table 5. Performance with fixed simulation time (here 4 s)

Test	Runtime with simulation [s]		Runtime of assessment [s]		Needed average sTDI [s]
	per cont.	total	per cont.	total	
I	0.415	71.35	0.084	14.52	0.755
II	0.465	79.92	0.074	12.85	0.650
III	0.510	87.76	0.061	10.43	0.428
IV	13.23	4620.2	0.073	25.4	0.206

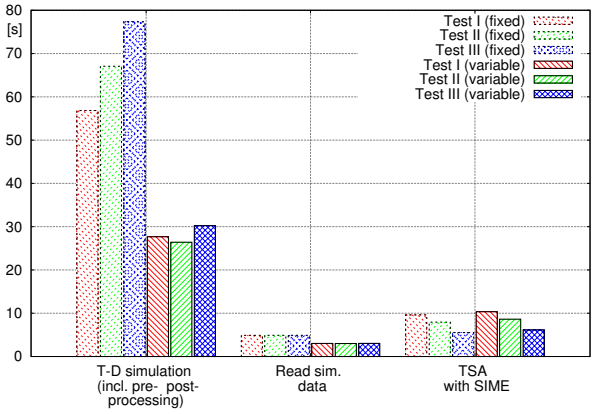

(a) Test $I - III$

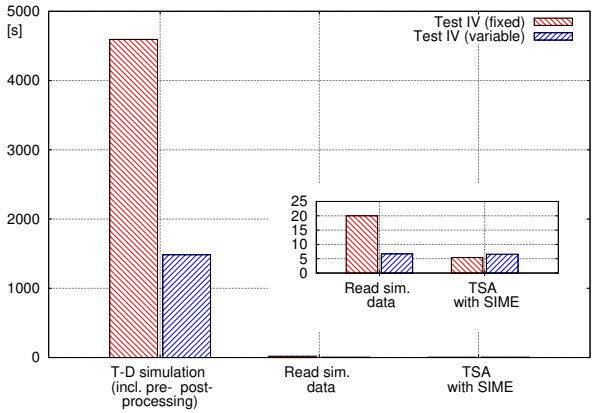

(b) Test IV with magnified detail.

Figure 6. Comparison of the runtime of the major parts of the screening method with fixed and variable simulation time

Without the simulation, the total runtimes are in the range of 10.43 s to 14.52 s corresponding to $61 - 84$ ms per contingency. In the large scale Test IV, the average runtime (incl. T-D simulation) per contingency is 13.23 s. This runtime per contingency is tremendously reduced to 73 ms, if only the runtime for the TSA is considered. In Fig. 6a, the dashed boxes show the runtime of the Tests $I - III$ split into three parts, namely time-domain simulation, which includes the time of data preparation and post-processing, reading of simulation data and stability assessment. The graph shows that around $80 - 90$ % of the runtime is spend on the time-domain simulation in the small

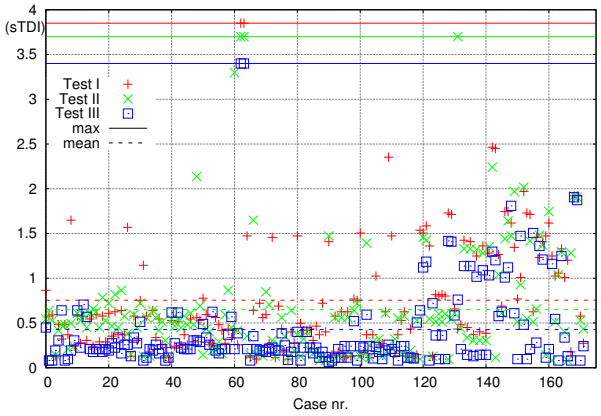

Figure 7. Test $I - III$ - Seconds of Time-Domain Integration (sTDI) required from fault clearance and until stability determination

test system. The same split of runtime for the large-scale system is shown in Fig. 6b (red hatched boxes). In this test, the time spend on the simulation corresponds to ca. 99 % of the total run-time. The magnified detail in the graph shows the runtime of the two other parts. These results show that a variable simulation time has a large potential for reducing the total runtime, which is enabled through an early stability prediction with SIME and, hence, an early simulation stop.

In [8], it was proposed to measure the performance of SIME based methods in needed seconds of time-domain integration (sTDI) until determination of stability. The sTDI's for each contingency and the Tests $I - III$ are shown in Fig. 7 and the needed average for each test was presented in Table 5. In the graph the average simulation time needed is indicated by a horizontal dashed line, the maximum simulation time by a solid line and the colors indicate the corresponding test. The graph shows that in the majority of the cases a simulation time of less than a second is sufficient and that there are only very few cases, where the maximum simulation time was reached.

Performance with variable simulation time: In the previous section, it was shown that time-domain simulation with fixed simulation time is dominating the runtime of the screening method. In order to further speed up the screening, the three tests were conducted with variable simulation time, where the simulation is stopped once the TSA method has determined stability of the currently investigated case. Hence, the simulation time of the individual cases correspond to the sTDI, shown in Fig. 7, plus pre-fault simulation and fault clearing time (here 100 ms and, depending on the test, 50, 200 or 500 ms respectively).

Table 6 shows the runtime of the four tests of the screening method with variable simulation time. The results reveal that this leads to considerable shorter runtimes in the first setup, where the time-domain simulations were included. In Tests $I - III$, the runtimes are reduced by around 43 % to 51 % and are in the range of $39.42 - 41.06$ s for the assessment of the 172 contingencies. In the test on the large-scale system, the gain due to the variable simulation time becomes even more visible, since the runtime was decreased by 67 % to 1497.5 s. It should be noticed that it also led to shorter runtimes for the setup without time-domain simulation, which is due to a reduction of the time needed to read the simulation data.

The figures in Fig 6 show a comparison of the runtimes with fixed and variable simulation time. The graphs show as expected that the main runtime reduction stems from the reduced time spent on time-domain simulations. Firstly, it is noticeable that

Table 6. Performance of fast screening method with variable simulation time

Test	Runtime with simulation [s]		Runtime of assessment [s]		Needed average
	per cont.	total	per cont.	total	sTDI [s]
I	0.239	41.06	0.078	13.38	0.755
II	0.221	38.03	0.067	11.62	0.650
III	0.229	39.42	0.053	9.19	0.428
IV	4.29	1497.5	0.038	13.3	0.206

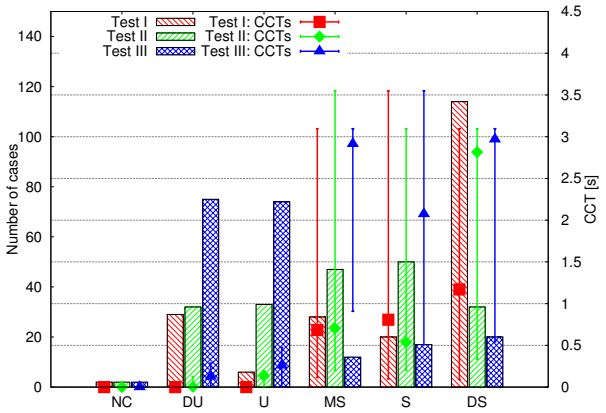

Figure 8. Fault ranking results: Bar graph (left y-axis) indicates number of cases in a particular category and test. The data points and error bars show average and range of CCTs in the corresponding category and test (right y-axis).

the reduction is significant in particular in the large-scale Test IV and Test III with a clearing time of 500 ms, where there is a larger number of unstable cases. This can be explained by the shorter simulation of the system response due to the application of the early stop criteria, described in Sec. 2.4.4. Secondly, a reduction of the time needed to read the simulation data is noticeable and this results from the lower number of simulation data, which was already mentioned earlier. Finally, it should be noted that the time needed for the TSA using SIME is not affected by the variation of the simulation time, which was expected.

3.2.4 Classification of faults The bar graph in Fig. 8 summarizes the results of the classification of the contingencies as proposed in Sec. 2.4.5. It should be mentioned that in this section only the results of the contingencies are depicted, which were correctly assessed by the proposed assessment method. The different contingency categories are shown on the x-axis. The number of identified contingencies in each test in the respective category are displayed by the bars belonging to the left y-axis. The bar graph shows that with longer clearing times the number of definitely unstable (DU) as well as unstable (U) cases increases and vice versa the number of definitely stable (DS) cases increases with shorter clearing times. Moreover, it should be noticed that the number of marginal stable (MS) cases peaks in the test with intermediate clearing time. These results are in good agreement with intuition. It should be mentioned, that independent of the fault clearing time two cases always were identified as not classifiable (NC). These are corresponding to faults that lead to islanding, where one island consists of one generator and a load. In such a case, stability can not be determined as mentioned earlier.

The data points in Fig. 8 depict the average critical clearing times (CCTs) of the contingencies in the respective categories and tests (shown on the right y-axis). Furthermore, an error bar is added to each average critical clearing time, which stretches from the minimum to the maximum CCT in the respective category and test. It should be noted that the algorithm used to identify CCTs stopped the search for CCTs when the clearing time became larger than 3 s. It is assumed that these cases are stable in the during fault as well as post fault condition. The CCTs of the contingencies in the unstable categories (DU + U) are, as expected, always below the respective actual clearing times (50/200/500 ms). Furthermore, it can be observed, that the average clearing time in the category DU is lower than in the category U, which confirms the effectiveness of the categorization. The results obtained for the stable cases and categories (MS, S, DS) are less clear. The maximum and minimum CCTs in each stable category vary greatly. However, it may be argued that a general upward trend can be observed for the average CCTs from DU to DS, when ignoring outliers such as the few MS cases in Test III, which correspond to only 3 % of the correctly assessed cases. The upward trend of the CCTs indicates again the effectiveness of the proposed classification. The problem of precisely classifying the stable cases may be explained by the difficulty to determine the correct critical group of machines. A new method or criterion, which enables early and accurate identification of this critical group, could considerably improve the classification results of stable cases. Finally, it should be mentioned that the categories are not intended to strictly split the contingencies with respect to their CCTs, but allow a categorization relative to the fault clearing time and the disturbance's severity in the current system condition.

4 Conclusion

In this paper a framework for on-line contingency screening for transient stability assessment is presented. The method aims at providing a classification of the stable as well as the unstable cases with respect to their severity. It uses a system snapshot, assumed to be provided by PMUs, and data from a corresponding model database to determine the current admittance matrix of the system. For each considered contingency the admittance matrix is modified to represent the post-fault condition and a graph theory based approach is used to identify islanding. If islands are detected, it is assessed which generators and loads are in the individual islands. The system snapshot is used to initialize a time-domain simulation, where a particular contingency is applied. The stability of each case is evaluated employing SIME and the assessment is stopped once the early stop criteria are fulfilled. Furthermore, each contingency is categorized with information extracted from the $P_a(\delta)$ curve of the OMIB system. The accuracy and speed of the method was tested on a small and a real-life large-scale test system. Four tests with different fault clearing times were carried out. The accuracy assessment showed a very high success rate with respect to stability assessment. It was shown, that the proposed method filters between $89 - 98$ % of the stable cases and correctly identifies $96 - 100$ % of the unstable cases. Consequently, the method is slightly more conservative, which is preferable for a screening method. The assessment of the runtime exposed that the majority of the CPU time is spent on the time-domain simulation and it was shown that by introducing a variable simulation time a considerable speed up could be achieved. The proposed method was compared with the original SIME method and it was shown that the probability of Type-I errors could be halved. Finally, the results of the classification of contingencies were presented by comparing the results to the CCTs of the individual contingencies. This showed that the categorization approach is promising. However, it is expected that the results, particular for stable cases, could be further improved through an early and accurate identification of the correct critical and non-critical group of gen-

erators. As a future extension, we will combine our methodology with possibilities to further speed up time-domain simulation through the use of parallelization and equivalencing techniques or simplified representation of the external system (such as the one recently proposed in [25]).

References

[1] F. Li, W. Qiao, H. Sun, H. Wan, J. Wang, Y. Xia, Z. Xu, and P. Zhang, "Smart Transmission Grid: Vision and Framework," *IEEE Transactions on Smart Grid*, vol. 1, no. 2, pp. 168–177, Sep. 2010.

[2] S. C. Savulescu, *Real-Time Stability in Power Systems.* New York: Springer Verlag, 2006.

[3] Working Group Cigré C4.601, "Review of on-line dynamic security assessment tools and techniques," Cigré, Paris, France, Tech. Rep. June, 2007.

[4] C. Fu and A. Bose, "Contingency Ranking Based on Severity Indices in Dynamic Security Analysis," *IEEE Transaction on Power Systems*, vol. 14, no. 3, pp. 980–986, Aug. 1999.

[5] V. Chadalavada, V. Vittal, G. C. Ejebe, G. D. Irisarri, J. Tong, G. Pieper, and M. McMullen, "An On-Line Contingency Filtering Scheme for Dynamic Security Assessment," *IEEE Transaction on Power Systems*, vol. 12, no. 1, pp. 153–161, Feb. 1997.

[6] M. Benidris, N. Cai, and J. Mitra, "A fast transient stability screening and ranking tool," *Proceedings - 2014 Power Systems Computation Conference, PSCC 2014*, Aug. 2014.

[7] Y. Xue, T. Huang, and F. Xue, "Effective and Robust Case Screening for Transient Stability Assessment," in *2013 IREP Symposium Bulk Power System Dynamics and Control - IX Optimization, Security and Control of the Emerging Power Grid*, Rethymnon, Greece, Aug. 2013, pp. 1–8.

[8] M. Pavella, D. Ernst, and D. Ruiz-Vega, *Transient Stability of Power Systems: A Unified Approach to Assessment and Control.* Boston/Dordrecht/London: Kluwer Academic Publishers, 2000.

[9] B. Lee, S.-H. Kwon, J. Lee, H.-K. Nam, J.-B. Choo, and D.-H. Jeon, "Fast contingency screening for online transient stability monitoring and assessment of the KEPCO system," *IEEE Proc., Gener. Transm. Distrib.*, vol. 150, no. 4, pp. 399–404, Jul. 2003.

[10] C.-W. Liu, M.-C. Su, S.-S. Tsay, and Y.-J. Wang, "Application of a Novel Fuzzy Neural Network to Real-Time Transient Stability Swings Prediction Based on Synchronized Phasor Measurements," *IEEE Transactions on Power Systems*, vol. 14, no. 2, pp. 685–692, May 1999.

[11] F. Hashiesh, H. E. Mostafa, A. R. Khatib, I. Helal, and M. M. Mansour, "An intelligent wide area synchrophasor based system for predicting and mitigating transient instabilities," *IEEE Transactions on Smart Grid*, vol. 3, no. 2, pp. 645–652, 2012.

[12] T. L. Vu and K. Turitsyn, "A Framework for Robust Assessment of Power Grid Stability and Resiliency," *IEEE Transactions on Automatic Control*, vol. 62, no. 3, pp. 1165–1177, Jun. 2016.

[13] J. Mitra, M. Benidris, and Niannian Cai, "Use of homotopy-based approaches in finding Controlling Unstable Equilibrium Points in transient stability analysis," in *2016 Power Systems Computation Conference (PSCC).* IEEE, Jun. 2016, pp. 1–7.

[14] M. Oluic, M. Ghandhari, and B. Berggren, "Methodology for Rotor Angle Transient Stability Assessment in Parameter Space," *IEEE Transactions on Power Systems*, vol. 32, no. 2, pp. 1202–1211, May 2016.

[15] T. Weckesser, H. Jóhannsson, S. Sommer, and J. Østergaard, "Investigation of the Adaptability of Transient Stability Assessment Methods to Real-Time Operation," in *IEEE Proc., Innovative Smart Grid Technologies*, Berlin, Germany, Oct. 2012, pp. 1–9.

[16] H. Morais, P. Vancraeyveld, A. Pedersen, and M. Lind, "SOSPO - SP: Secure Operation of Sustainable Power Systems Simulation Platform for Real - Time System State Evaluation and Control," *IEEE Transactions on Industrial Informatics*, vol. 10, no. 4, pp. 2318–2329, May 2014.

[17] M. Glavic and T. V. Cutsem, "Tracking network state from combined SCADA and synchronized phasor measurements," in *2013 IREP Symposium Bulk Power System Dynamics and Control - IX Optimization, Security and Control of the Emerging Power Grid*, Rethymno, Greece, Aug. 2013, pp. 1–10.

[18] T. Weckesser, H. Jóhannsson, and J. Østergaard, "Impact of Model Detail of Synchronous Machines on Real-time Transient Stability Assessment," in *2013 IREP Symposium Bulk Power System Dynamics and Control - IX Optimization, Security and Control*

of the Emerging Power Grid, Rethymnon, Greece, Aug. 2013.

[19] J. Kleinberg and E. Tardos, *Algorithm Design*, M. Suarez-Rivas, Ed. Boston: Pearson Addison Wesley, 2006.

[20] M. Glavic, D. Ernst, D. Ruiz-Vega, L. Wehenkel, and M. Pavella, "E-SIME - A Method for Transient Stability Closed-Loop Emergency Control : Achievements and Prospects Fundamentals of E-SIME," in *2007 iREP Symposium- Bulk Power System Dynamics and Control - VII, Revitalizing Operational Reliability*, Charleston, USA, Aug. 2007.

[21] G. Rogers, *Power System Oscillations*. New York, USA: Kluwer Academic Publishers, 2000.

[22] A. Semerow, S. Hohn, M. Luther, W. Sattinger, H. Abildgaard, A. D. Garcia, and G. Giannuzzi, "Dynamic Study Model for the interconnected power system of Continental Europe in different simulation tools," in *2015 IEEE Eindhoven PowerTech*. Eindhoven, Netherlands: IEEE, Jun. 2015, pp. 1–6.

[23] P. Kundur, *Power System Stability and Control*, N. J. Balu and M. G. Lauby, Eds. New York, USA: McGraw-Hill Inc., 1994.

[24] D. Fabozzi, B. Haut, A. S. Chieh, and T. Van Cutsem, "Accelerated and Localized Newton Schemes for Faster Dynamic Simulation of Large Power Systems," *IEEE Transactions on Power Systems*, vol. 28, no. 4, pp. 4936–4947, Mar. 2013.

[25] S. Kim and T. J. Overbye, "Mixed Transient Stability Analysis Using AC and DC Models," *IEEE Transactions on Power Systems*, vol. 31, no. 2, pp. 942–948, Mar. 2016.

Acknowledgment

The Version of Record of this manuscript has been published and is available in Electric Power Components and Systems 02 May 2017:
http://www.tandfonline.com/10.1080/15325008.2017.1310953.